Correlation of Surface Pressure and Vortical Flow Structures in an Unsteady Separating Flow

Stephen Snider*, Daniel Morse*,
Sourabh V. Apte†, and James A. Liburdy‡
Oregon State University, Corvallis, OR, 97331, USA

Controlling flow in an unsteady separating flow requires accurate information about the surface forces and the effect that vortical structures in the flow field have on those surface forces. A correlation between vortex passage and surface pressure is defined to determine appropriate locations for sensors on the surface of a square cylinder for control feedback. Data are generated using a large eddy simulation of flow over a square cylinder at Reynolds number of $21,000$. The flow is decomposed using proper orthogonal decomposition (POD) based on the frequency and energy content of the velocity and pressure fields around the square cylinder. Two data sets are reconstructed from the POD: (i) the first two modes containing approximately 75% of the energy of the flow and representing the large scale wake oscillation, and (ii) higher order modes containing the remainder of the energy of the flow representing smaller scale features in the flow, such as those shed from the leading edge. Vortex detection using the Γ^* function is performed on both data sets, where the Γ^* function is an area-averaged measure of the swirl around each point in the flow. Vortices in the data set composed of the first two modes tend to be large scale features and oscillate with the same frequency as the bluff body wake oscillation. The vortices detected in the higher order modes are smaller and tend to be the vortical structures shed from the leading edge of the square cylinder and convected downstream. In both data sets, the correlation values increase from the leading edge to the trailing edge, indicating that the downstream half of the square cylinder is most affected by vortical structures in the flow. Based on the correlation values, the segments of the square cylinder surface closest to the trailing edge would be best for sensor location to provide input for flow control.

Nomenclature

$a_k(t)$	POD amplitude function
A_M	Search area for Γ^*
C_p	Pressure coefficient
$\mathscr{C}^j_{P_s\Gamma^*}$	Correlation value
d	POD function of velocity and pressure
$I_{\mathscr{C}}$	Integral scale
$f_k(x)$	POD spatial modes
N_{s_i}	Number of surface points per segment
N_t	Number of time steps
P	Pressure, N/m^2
S_j	Segment on cylinder surface
St	Strouhal number
t^*	Time scale
u	Velocity, m/s
x	Variable value vector
Γ^*	Gamma Function
λ	Distance from cylinder surface

*Graduate Student, School of Mechanical, Industrial, and Manufacturing Engineering, 204 Rogers Hall, Corvallis, OR 97331, and AIAA Member.
†Assistant Professor, School of Mechanical, Industrial, and Manufacturing Engineering, 204 Rogers Hall, Corvallis, OR 97331.
‡Professor, School of Mechanical, Industrial, and Manufacturing Engineering, 204 Rogers Hall, Corvallis, OR 97331, and AIAA Member.

ν Kinematic viscosity, m^2/s
ρ Density, kg/m^3
Subscript
i Variable number
j Surface segment number
k POD mode number
s_i Surface segment point number
∞ Free stream value

I. Introduction

This study examines a method of identifying how to best determine the most effective sensor location for a feedback control scheme used to provide flow control for unsteady flow separation. The flow phenomena under consideration consists of a flow instability resulting from leading edge separation. Large scale flow structures, typical in the form of vortical flow elements, emanate from the leading edge and are convected downstream. These flow elements can result in unsteady forcing on the surface of the body resulting in surface pressure oscillations. In a feedback control system a sensor output to this surface pressure forcing may be appropriate to use for actuation of flow control to limit the surface forcing oscillations. Therefore, it is necessary to understand the flow physics associated with the occurrence of large scale vortical flow elements and how they are correlated with the surface pressure transients. The application of this technique may provide a means of identifying the surface locations that provide the most apparent correlation between surface pressure and large scale vortical structures that result in pressure fluctuations.

In this study a numerical simulation of the flow around a square cross section cylinder is used to provide the data set. This flow provides a leading edge separation and also a trailing edge separation resulting in time dependent pressure distributions on the cylinder surface. A large eddy simulation is performed with at a cylinder Reynolds number of $21,000$ resulting in periodic vortex shedding. The resultant velocity field is then analyzed using a vortex detection scheme and the vortical structures are tracked in space and time. The results also provide the detailed pressure field, where here the surface pressure is of interest in how it correlates with the vortical structure dynamics.

II. Background

Traditionally, flow analysis involving turbulence and unsteady coherent structures that may be imbedded within the broad spectrum of turbulence has been based on collecting one-point and two-point statistics. However, there is a large and growing literature on swirl and vortical flow detection methods.[4–7] Proper Orthogonal Decomposition (POD),[6] the λ_2 (second eigenvalue) method,[4,8] and the Γ^* function,[7,9] among others, have been proposed and typically used for flow analysis. Specific identification of vortex structures (or pressure minima)[4,8,9] and correlating vortex shedding to leading edge separation,[3] have been applied.

Previous works have examined the ability of vortex detection methods to detect multiple scales of vortices[14] shed in separating flow. It is shown that the Γ^* function and the λ_2 method tend to detect flow features very well at all scales, with the Γ^* function detecting larger features slightly better than the λ_2 method and the λ_2 method detecting smaller vortex cores slightly better than the Γ^* function. The vortex detection methods have also been applied to temporally evolving flows[15] and were found to be useful in detecting and tracking vortical structures over time.

Flow over a square cylinder at $Re \approx 21,000$, based on the inlet velocity ($U_\infty = 0.3318$ m/s), the square cylinder size (L = 1 m and the fluid kinematic viscosity ($\nu = 15.08 \times 10^{-6}$ m^2/s), is obtained using large eddy simulation. A three-dimensional simulation is performed with Dirichlet conditions at the inlet, a slip condition at the top and bottom surfaces, periodic conditions in the spanwise direction, and a convective boundary condition for the outlet. The large eddy simulation is performed based on a colocated grid, fractional step algorithm[10–12] to collect the velocity and pressure data in space and time. The flow solver has been validated with available experimental data for a variety of flow configurations involving separated turbulent flows and swirling regions.[11–13]

This data set was selected for a number of reasons. It represents leading edge flow separation with significant vortical flow structure development. The flow is at a reasonably high Reynolds number to assure a range of scales of motion and energy. Computationally obtained data sets are used because the computational simulation contains both velocity and pressure field results over the full extent of the field of interest, while experimental data will be limited to a velocity vector field (usually in two dimensions, and rarely more than two components). Consequently, experimental data sets lack the ability to use the pressure and/or the full dimensional field and its possible gradients as an indicator variable, or feature descriptor.

The paper is arranged as follows. In the next section the flow analysis techniques are described in detail. These include the Γ^* function calculation, Proper Orthogonal Decomposition (POD), and the development and calculation of the correlation value. These techniques are then applied to the square cylinder data set to correlate the passage of vortices with the surface pressure. From the correlation, segments on the cylinder surface with the highest correlation values are noted as potential locations for pressure sensors in a control system.

III. Flow Analysis Techniques

The Proper Orthogonal Decomposition (POD) is used to identify the periodic processes in the flow. The POD of the velocity and pressure fields are expressed as a single function of space and time, $d(x,t)$. This function can be approximated as the sum of the products of functions $a_k(t)$ and $f_k(x)$ where k is the mode number, shown in Equation 1.

$$d(x,t) \approx \sum_{k=1}^{M} a_k(t) f_k(x) \tag{1}$$

An NxM design matrix, D is constructed from the experimental data where N is the number of time steps and M is the number of data locations. In actuality, the u,v and P data are all considered in the same data set so that M is 3x the number of data locations. The components of D are $d(x,t)$ which are the experimental data points. A singular value decomposition of D provides the spatial modes, $f_k(x)$, and their associated amplitude time series, $a_k(t)$.

To relate the surface pressure to the large-scale vortical structures generated by the leading and trailing edge separations a two-point correlation function is necessary. The goal is to define a correlation function that identifies how the local surface pressure correlates with the large scale vortical structures as they are convected over the surface. To achieve this, the spatial correlation of the surface pressure versus a measure of the strength of the vortical structure is defined. A measure of the swirl strength defined by the Γ^* function is used:[7]

$$\Gamma^*(x,y) = \frac{1}{A_M}\int_{A_M} \frac{\left(\overline{PM}\times\overline{U}_M\right)\cdot\widehat{Z}}{\left(\|\overline{PM}\|\|\overline{U}_M\|\right)} dA = \frac{1}{A_M}\int_{A_M} \sin(\theta_M) dA, \tag{2}$$

where M are the discrete grid nodes within the sub-area, A_M. $\overline{PM}$ is the vector from center point P, to nodes M, and $\overline{U}_M$ is the velocity vector at grid nodes M. The unit vector, $\widehat{Z}$, associated with $\overline{PM}$ for the x $-$ y plane data is $\{0,0,1\}$. This is equivalent to the summation of the *sine* of the angle (θ_M) between the velocity vector at points within the area A_M and the position vector from these points to the position (x,y).

The larger the value of Γ^* the greater the local swirl component of the flow within area A_M. This criterion is used to identify a vortex motion within the flow, where Γ^* varies between -1 and 1, where the positive values correspond to counterclockwise and negative for clockwise rotation. Figure 1 shows the Γ^* field output at a single time step for the flow over the square cylinder at a Reynolds number of $21,000$. The contour plot is of the Γ^* function applied to the raw data set for flow over the square cylinder. Note the smaller features detected near the leading edges of the square cylinder as well as the large scale recirculation detected in the wake. Features of most interest are those above the top surface of the cylinder as those are expected to have more influence on the surface forces than vortices in the wake.

Computing the vortex swirl strength using the Γ^* function and knowing the surface pressure $P_s(\mathrm{x_s},\mathrm{t})$, a two-point correlation is proposed to detect the surface region that is predominantly influenced by the passing of vortical structures. Time series data are used to obtain this correlation by using each time step spatial data to determine the spatial correlation between surface locations and flow field data. In order to do this, the top surface is segmented into four equal length regions along the cylinder, and the correlation is obtained for each region. Correlations for each region are limited to the flow field projected vertically above each segment. These correlations then will be used to identify the locations on the surface that are most influenced by the convected large scale structures generated at the leading edge separation.

The correlation for each segment S^j is defined as:

$$\mathscr{C}^j_{P_s\Gamma^*}(\lambda) = \frac{1}{N_{s_i}}\frac{1}{N_t}\sum_{t=1}^{N_t}\sum_{i=1}^{N_{s_i}} \| \left(C_{p_{s_i}}(\vec{x}_{s_i},t) - \overline{C_{p_\infty}(\vec{x}_{s_i})}\right)\cdot\left(\Gamma^*(\lambda,t) - \overline{\Gamma^*(\lambda)}\right)\| \tag{3}$$

where $\vec{x}_{s_i}$ is a point on the surface such that $s_i \in S^j$, $\vec{x}$ is a point in the flow field, $\lambda = \|\vec{x}_{s_i} - \vec{x}\|$ is the separation distance between the two points, $C_{p_{s_i}}$ is the local pressure coefficient at the surface point, $\overline{C_{p_{s_i}}}$ is the time-averaged pressure coefficient at that point, Γ^* is the swirl strength parameter at the point in the flow field, $\overline{\Gamma^*}$ is the time-averaged swirl

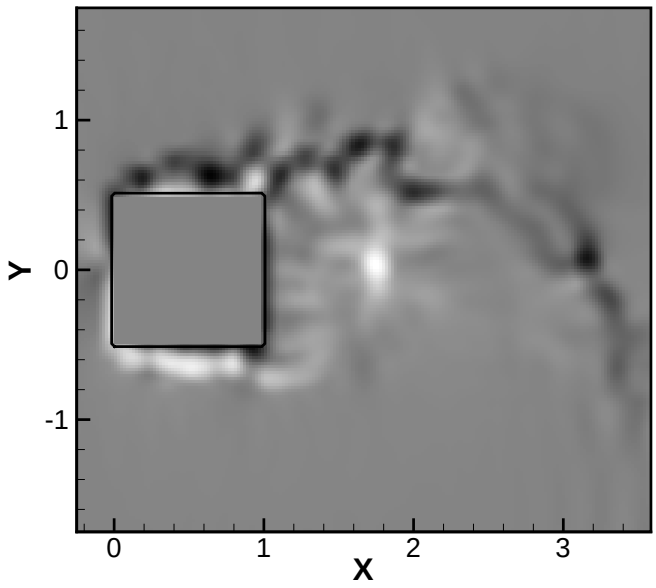

Figure 1. Contours of Γ^* function for flow over a square cylinder. Shown is the symmetry plane with a close-up view of the flowfield near the cylinder.

strength parameter at the point in the flow , N_{s_i} are the number of surface points that lie within the segment S^j, and N_t are the number of time frames.

Since the distance λ is restricted to a region directly above the segment S^j the correlation is being computed, the effect of vortices passing over that segment specifically are determined. This eliminates potentially unwanted results such as a correlation between vortices far downstream and local surface pressure changes.

A integral scale, $I_{\mathscr{C}} = \int_0^\infty \mathscr{C}^j_{P_s\Gamma^*}(\lambda)\mathrm{d}\lambda$, is derived from the correlation curves for each segment. The integral scale represents the cumulative effect of the swirl in the flow on the surface pressure. A larger value for the integral scale in a segment implies a stronger correlation between the vortical structures above that segment and the surface pressure, or a greater extent from the surface over which vortical structres impact the surface pressure.

IV. Results

The LES data set for flow over a square cylinder was evaluated using a velocity-based feature extraction technique. The Γ^* function has been used to detect vortical structures in two data sets that represent the reconstruction of the velocity field based on: (i) the first two modes and (ii) higher order modes from the POD analysis. From this vortex detection, the correlation between surface pressure and vortex passage is calculated for each data set.

A. LES Data on Flow Over a Square Cylinder

Figure 2 shows snapshots of velocity vectors and pressure contours for flow over a square cylinder at $Re \approx 21,000$ obtained from large eddy simulation. A total of around 4–million Cartesian grid points are used in the computational domain. The flow separates at the leading edge corners and forms an oscillatory wake downstream giving rise to large scale vortical structures containing large levels of turbulent kinetic energy. Two instants in time are shown in Fig. 2 (a-d) that highlight the extreme cases of the periodic flow. At $t^* = 141.68$ the wake is oscillating towards the bottom surface of the square cylinder. At this instant, the separation from the top surface is small, so the vortices shed from the leading edge remain close to the surface. In contrast, at $t^* = 145.99$ the wake is oscillating in the direction of the top surface, leading to a large separation above the top surface and vortices further from the surface.

Fig. 2 (e-f) compare the mean and RMS velocity profiles of the simulation data to experimental results[16,18] at a location $x/D = 1$ behind the downstream face of the square cylinder. Both the mean velocity profile and the RMS

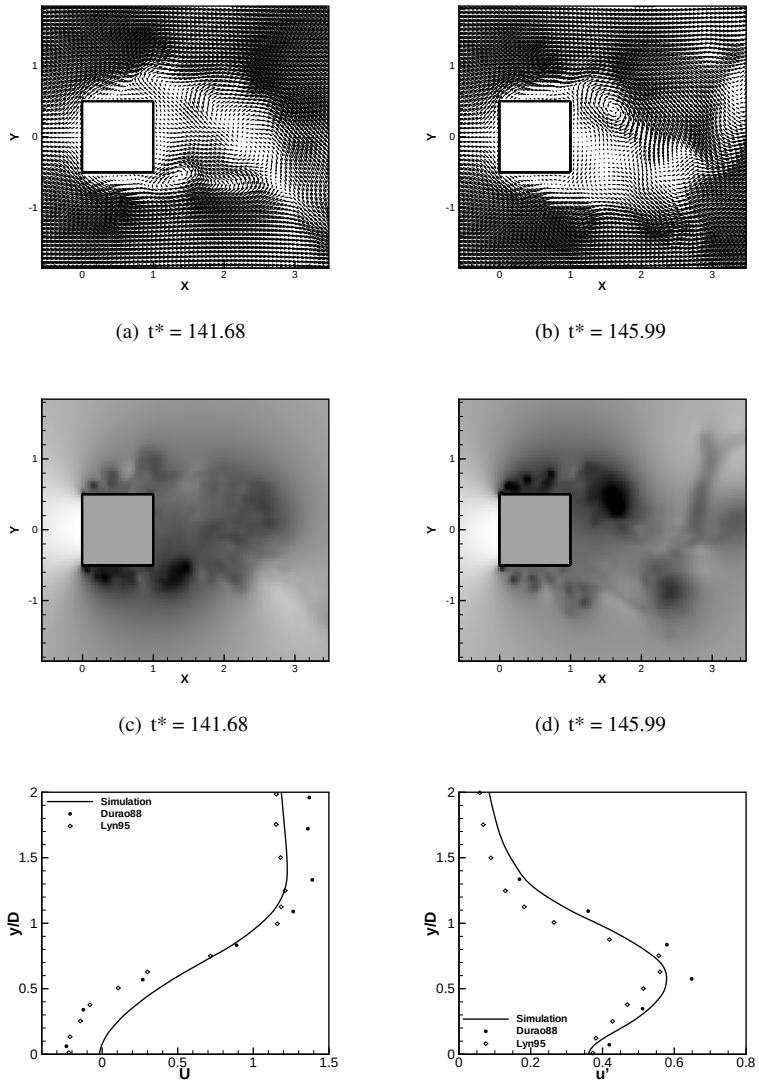

(a) t* = 141.68 (b) t* = 145.99

(c) t* = 141.68 (d) t* = 145.99

(e) $\overline{U}$ (f) u'

Figure 2. Large eddy simulation of flow over a square cylinder at $Re = 21,000$. (a-b) velocity vectors in the symmetry plane ($t^* = tU_\infty/L$), (c-d) pressure contours in the symmetry plane, (e) mean wake velocity profile at $x/D = 1$ from back cylinder face compared to experimental results,[16,18] (f) RMS velocity fluctuation profile at $x/D = 1$ compared to experimental.[16,18]

velocity fluctuations match the experimental results well.

The aforementioned large scale oscillation is apparent in a time probe of pressure taken at the midpoint of the top surface of the cylinder. Figure 3 shows this time probe and the corresponding spectral distribution. The Strouhal number $St = fL/U_\infty$ is 0.128, which matches well with experimental and simulation results for similar square cylinders.[16–18] Note that $t^* = 0$ in Fig. 3 denotes the beginning of data collection for vortex detection, not the beginning of the simulation.

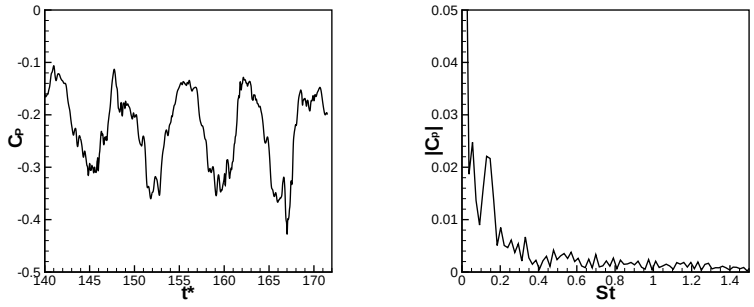

(a) (b)

Figure 3. Pressure signal at midpoint of top surface of square cylinder. (a) Time probe ($C_p = P/(\rho U_\infty)$), (b) spectral distribution ($St = fD/U_\infty$).

B. POD on Flow Over a Square Cylinder

The number of modes was limited to the number of timesteps, in this case 101. It was observed that the first two modes accounted for approximately 75% of the variance, or energy, of the velocity and pressure fields. The amplitude time series of these two modes were seen to be out of phase by $\pi/2$ and their frequency matches the bluff shedding observed in the simulation. Figure 4 is the amplitude time series for the most energetic mode, $k = 1$, and the first of the higher order modes, $k = 3$.

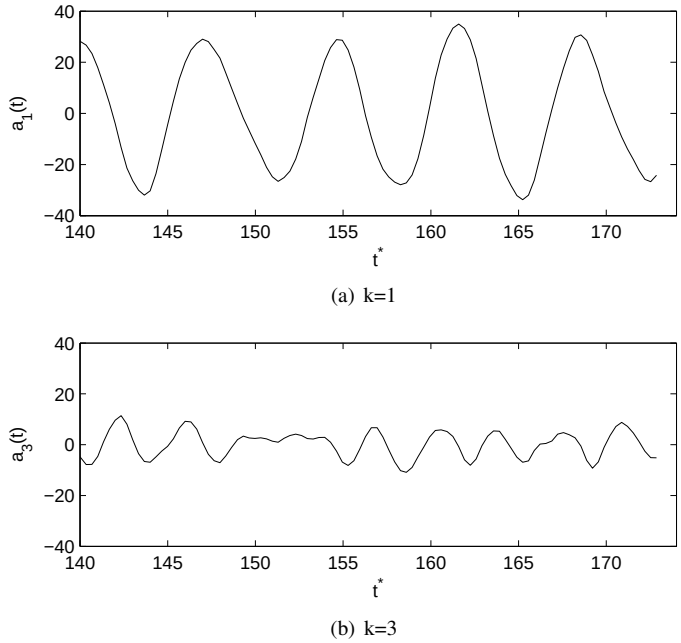

(a) k=1

(b) k=3

Figure 4. Amplitude time series plots for modes (a) $k = 1$ and (b) $k = 3$ from the Proper Orthogonal Decomposition.

The first mode, $k = 1$ from the POD analysis is periodic with a Strouhal number $St = 0.18$. This is higher than

the frequency shown in Fig. 3, but is still similar to the frequency of the large scale wake oscillation observed in flow over a square cylinder. Since the first mode contains about 70% of the energy of the flow, it is likely that the wake oscillation is the most energetic feature in the flow. The second mode time series (not shown) oscillates with the same frequency, but is out of phase with the first mode by $\pi/2$. Mode three and the higher order modes each contain less than 3% of the energy of the flow. The amplitude time series of mode three is periodic with Strouhal number $St = 0.30$, about twice that of the lower order modes. This higher frequency content is expected based on the vortex shedding from the leading edge, as opposed to the low frequency wake oscillation. From this, it is hypothesized that the third and higher order modes represent the vortex shedding from the leading edge, and the first two modes represent the large scale wake oscillation and related vortical structures.

After POD analysis to determine the energy content of the different modes, the data are reconstructed into two data sets. The first data set contains only the first two modes, $k = 1$ and $k = 2$, which is primarily the large scale wake oscillation and large scale features in the flow. This data set contains approximately 75% of the energy in the flow. The second data set reconstructed contains all of the higher order modes, $k = 3$ through $k = 101$. This data set contains the remainder of the energy in the flow and is thought to represent the smaller scale (hence lower energy) features shed from the leading edge of the square cylinder.

C. Γ^* Function on Flow Over a Square Cylinder

Figure 5 shows the result of selected time step Γ^* function vortex detection on the two data sets representing the low and high order modes of the POD analysis. Both data sets contain vortical structures above the surface of the square cylinder as well as in the wake. The low order modes show large scale oscillation due to the wake. The structures detected in the low order mode data contain most of the energy in the flow, but may not represent well what effect individual vortices shed from the leading edge have on the surface pressure.

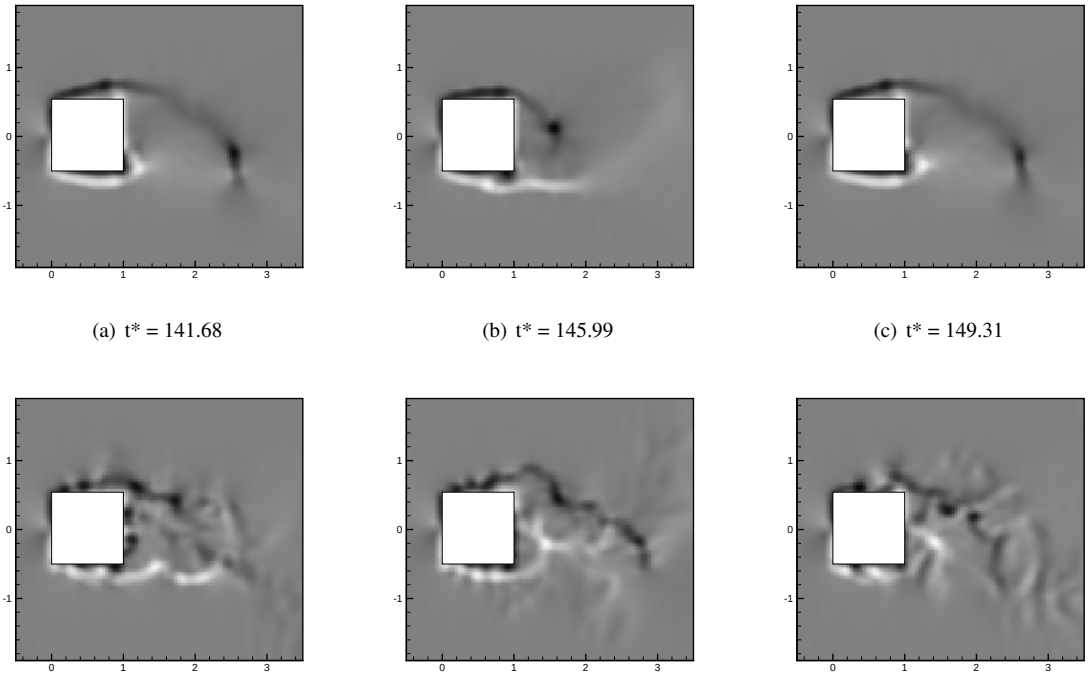

(a) t* = 141.68 (b) t* = 145.99 (c) t* = 149.31

(d) t* = 141.68 (e) t* = 145.99 (f) t* = 149.31

Figure 5. Contours of Γ^* function for flow over square cylinder. (a-c) first two modes of POD, (d-f) higher order modes of POD.

Vortical structures detected in the higher order modes, Fig. 5 (d-f), tend to be those that are shed from the leading edge of the square cylinder. These smaller structures remain close to the cylinder surface, so are expected to have a measureable effect on the surface pressure. It is observed that in the data of the higher order modes, the wake oscillation is still present, but has a reduced effect on the size of separation and path of vortices shed from the leading edge.

D. Correlation of Surface Pressure and Vortex Passage

Although the correlation is defined as a temporally averaged value, it is also instructive to look at how the correlation curves change as a function of space at fixed instants in time. This will give an indication of what features in the flow cause peaks in the correlation values and their locations in both the first two modes and the higher modes. Figure 6 shows the correlation values as a function of the distance from the cylinder surface for two instants in time for the first two modes as well as the higher order modes. Also shown are the contours of Γ^* above the top surface of the cylinder so the location of the peak correlation values can be compared to the location of vortical structures.

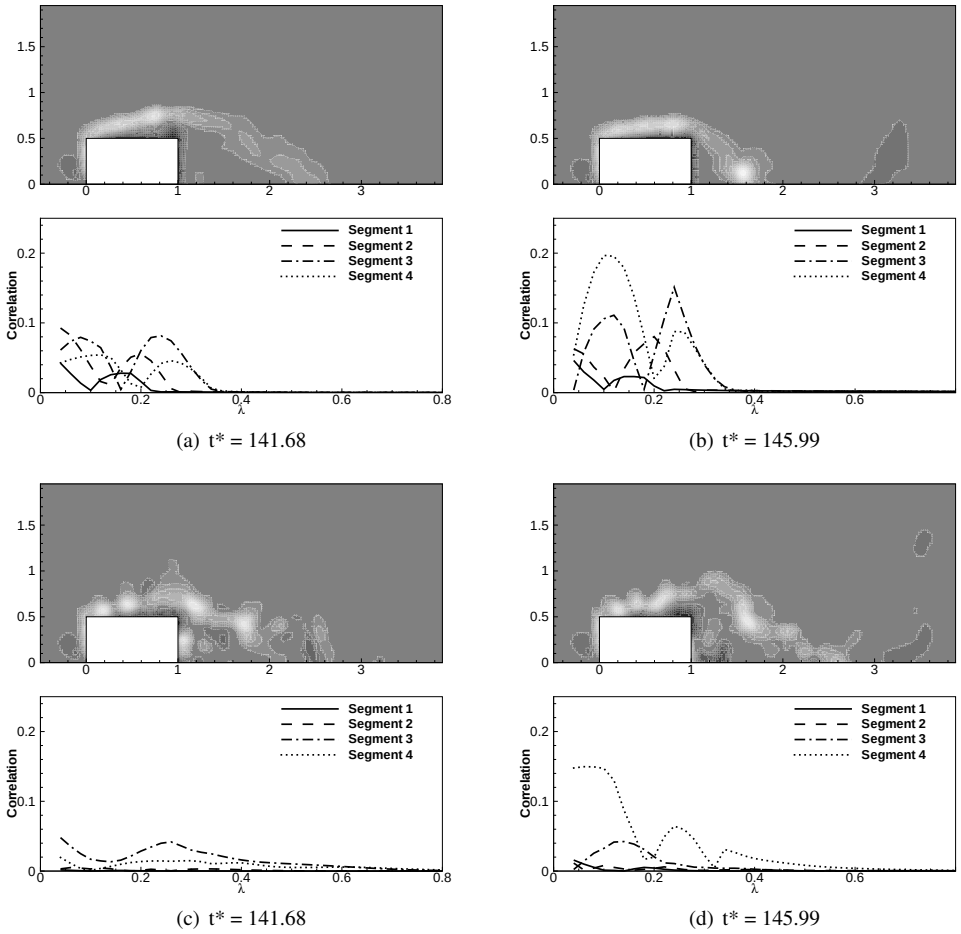

(a) t* = 141.68 (b) t* = 145.99

(c) t* = 141.68 (d) t* = 145.99

Figure 6. Correlation curves as a function of distance from cylinder surface and contours of Γ^* at the same instants in time. (a-b) modes 1 and 2 POD reconstruction, (c-d) higher order modes POD reconstruction.

From Fig. 6, peaks in the correlation values correspond to the center of detected vortical structures. The peak close to the surface corresponds to the wall layer, while the second peak corresponds to swirl in the free shear layer. The magnitude of the peaks tends to be higher for the segments close to the trailing edge of the cylinder. This indicates that the vortex passage has a larger effect on the surface pressure in these two segments than in the segments near the leading edge. Also note that these plots represent the *magnitude* of the correlation values. The sign of the correlation is affected solely by the direction of the swirl in the flow.

Based on the spatial correlation curves, a integral scale is defined as the integration of the correlation curve in each segment. This integral scale will privode insight into which segments are most affected by vortex passage and the strength and spatial extent of this interaction. Figure 7 shows a time probe of the integral scale for the first two modes and the higher order modes. Here only time traces for segment 3 are plotted; the other segments of the cylinder surface exhibit the same general behavior. In the low modes, Fig. 7 (a), the signal is strongly periodic due to the large scale wake oscillation. The higher modes may show some influence from the wake oscillation, but the time signal conains a broader frequency content with more amplitude variation.

The time traces were analyzed for frequency content which is shown in Figure 8. These data are based on the

absolute value of a periodic signal, so the frequency of the signal will be double that of the raw signal. In the low order modes the peak frequency, corresponding to a Strouhal number of approximately 0.30, correspond to the wake oscillation frequency observed in Fig. 3(b) and Fig. 4(a). The secondary peak in the spectrum distribution of the low modes corresponds to the frequency of mode three of the POD, Fig. 4(b). The spectrum distribution of the higher order modes, Fig. 8(b), shows a weak peak at a frequency that is close to that of the vortex shedding frequency in Fig. 4(b). The dominant wake frequency does not appear.

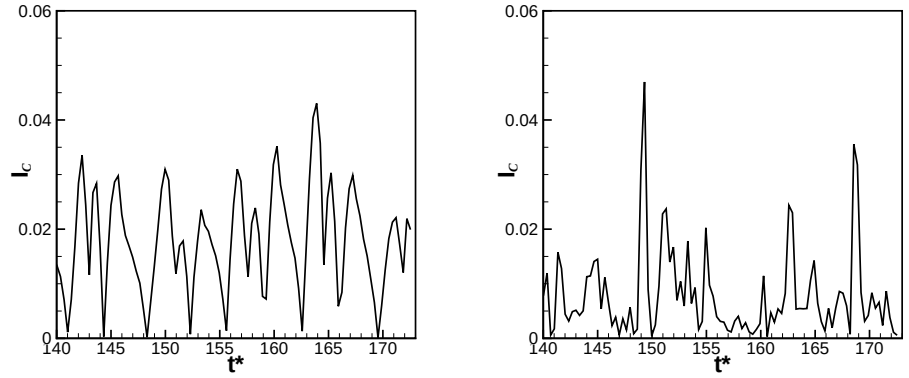

Figure 7. Segment 3 integral scale time probe. (a) first two modes POD reconstruction, (b) higher order modes POD reconstruction.

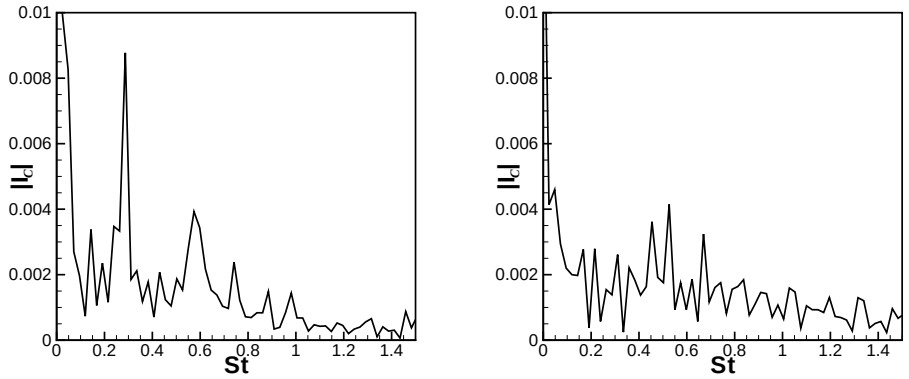

Figure 8. Segment 3 integral scale spectrum distribution. (a) first two modes POD reconstruction, (b) higher order modes POD reconstruction.

All of the instantaneous corelations were averaged for each segment and are shown in Figure 9. In the low order modes, there are two peaks in each segment. The first peak corresponds to vortices near the surface of the square cylinder, while the second peak corresponds to swirl in the free shear layer. The distance of the peak from the surface increases from the leading edge segment to the trailing edge segment because of the growth of the separated region. Note that while the second peak in the correlation curves is of lower magnitude than the peak close to the cylinder surface, the correlation value is still high, indicating that features in the shear layer have a large effect on the surface pressure.

The higher order modes average correlation have two weak peaks in the segments closest to the leading edge, shown in Fig 9 (b), but in segments three and four (near the trailing edge) the correlation value is highest near the wall and tends to be reduced with increasing distance from the surface. These curves highlight the extent of the separated region in the higher order modes data set, and show that events close to the cylinder surface tend to have the most effect on the surface pressure, although the surface pressure is obviously affected by the entire separated region.

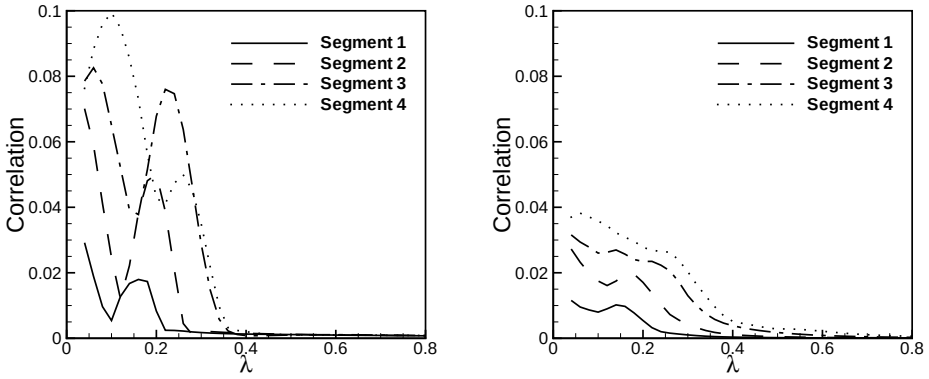

Figure 9. Time average correlation in each segment for: (a) reconstruction of first two modes from POD; (b) reconstruction of higher order modes from POD

To better quantify the total correlation in each segment over time, Figure 10(a) shows the time average values of the integral scale, $I_{\mathscr{C}}$, in each segment for the low and high modes reconstruction from POD. The correlation integral scales increase from the leading edge segment to the trailing edge segment. In the low order modes, the two segments closest to the trailing edge have a similar value for the correlation integral scale, indicating that the correlation values in the lower order modes are likely dominated by wake effects, which have a lower effect on the leading edge segments of the square cylinder.

The idea that the wake effects dominate the correlation integral scale is reinforced when the integral scale of the lower order modes is compared to those of the higher order modes. The integral scale increases steadily in the higher order modes, with a sharp rise in segment four. The increase in the integral scale is due to two factors: the increase in the magnitude of Γ^*_{RMS} and the increase in the distance from the surface of the peak values in the Γ^*_{RMS}. These two features are shown in Fig. 10(b) and (c). In the low order modes, the large increase in the integral scale values in segments three and four are due mainly to an increase in the magnitude of Γ^*_{RMS}. Likewise, the increase in the integration scale between segments three and four in the low order modes is due to an increase in the magnitude of Γ^* fluctuations near the cylinder surface.

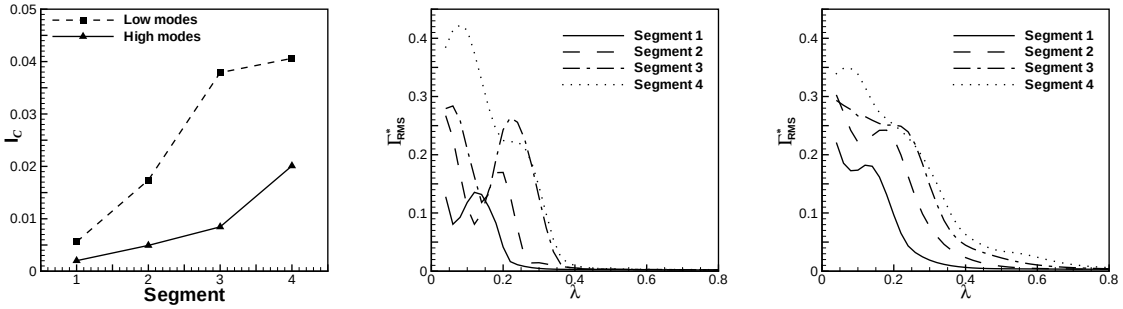

Figure 10. (a)Time average integral scale in each segment for low and high mode reconstruction from POD. RMS values of Γ^* for (b) first two modes reconstruction from POD, (c) higher order modes.

V. Conclusion

Large eddy simulation of flow over a square cylinder has been performed for the purpose of correlating vortex passage to surface pressure. Proper orthogonal decomposition is used on the LES results to decompose the flow field

based on the frequencies and energy content of the velocity and pressure in the flow. It is found that the first two modes of the POD contain approximately 75% of the energy in the flow. These modes correspond to the large scale wake oscillation and resulting vortical structures. Modes three through 101 of of the POD correspond to smaller structures in the flow, such as those shed from the leading edge.

Two data sets are reconstructed from the POD analysis, one that contains the first two modes of the POD, and one which combines the higher order modes. Vortex detection using the Γ^* function is performed on both data sets. It is found that the first two modes contain large scale features that are primarily in the wake. The vortices detected in the first two modes tend to oscillate with the same frequency as the wake. Vortical structures in the higher order modes are smaller and tend to be those shed from the leading edge, as well as small vortices in the wake. These smaller features tend to travel in a consistent path from the leading edge, along the separated region, and downstream into the wake. The features gain energy as they are convected downstream.

A correlation is defined which links vortical structures in the flow above the surface of a square cylinder to the pressure on the surface. In the low order modes, the correlation contains two peaks: one peak near the surface in the wall layer, and a second peak in the free shear layer. It is observed that the segments near the trailing edge have the highest correlation values due to the proximity of the wake and the domination of wake oscillation in the low order modes.

The correlation curves in the higher order modes tend to have peak values near the surface; the value of the correlation is reduced as distance from the surface increases. The surface segment with the highest correlation is the segment closest to the trailing edge, possibly due to wake effects in the higher order modes, but also due to the increase in energy in the vortical structures as they are convected downstream from the leading edge.

The results of the correlation indicate that sensors for controller feedback should be placed on the surface in the segments closest to the trailing edge but not so far downstream so as to be dominated by wake effects. Both the low modes and high modes show the highest correlation values in these segments, indicating that the trailing edge is most affected by the passage of vortical structures.

The analysis methods developed in this study are also applicable to other flows that may generate large wake effects. This includes airfoils at high angle of attack, flow over bluff bodies, and airfoils undergoing flapping motion.

Acknowledgments

The work is partially supported by AFOSR and ONR. James Liburdy and Daniel Morse thank AFOSR for partial support under the grant FA-9550-05-0041. Sourabh Apte and Stephen Snider thank ONR for partial support under the grant N000140610697. Computations were performed on the San Diego Supercomputing Center's Datastar machine.

References

[1]Hoarau, Y. Braza, M., Ventikos, Y., Faghani, D., and Tzabiras, G., " Organized Modes and the Three Dimensional Transition to Turbulence in the Incompressible Flow Around a NACA0012 Wing," *J. Fluid Mech.*, Vol. 496, 2003, pp. 63–72.

[2]Nishimura H., and Taniike, Y., "Aerodynamic Characteristics of Fluctuating Forces on a Circular Cylinder," *J. Wind Eng. Ind. Aerodynamics*, Vol. 89, 2001, pp. 713–723.

[3]Sicot, C., Auburn, S., Loyer, S., and Devinant, P., "Unsteady Characteristics of the Static Stall of an Airfoil Subjected to Freestream Turbulence Level Up to 16%", *Exp. in Fluids*, Vol. 41, 2006, pp. 641–648.

[4]Jeong, J. and Hussain, F., "On the Identification of a Vortex," *J. Fluid Mech.*, Vol. 285, 1995, pp. 69–94.

[5]Burgmann, S. and Brucker, C. and Schroder, W., "Scanning PIV Measurements of a Laminar Separation Bubble," *Exp. Fluids*, Vol. 41, 2006, pp. 319–326.

[6]Weiland, C. and Vlachos, P., "Analysis of the Parallel Blade Vortex Interaction with Leading Edge Blowing Flow Control Using the Proper Orthogonal Decompositions," Proceedings FEDSM2007, Joint ASME/JSME Fluids Engineering Conf. July, San Diego, 2007.

[7]Dano, B and Liburdy, J., "Vortical Structures of a 45^0 Inclined Pulsed Jet in Crossflow," AIAA 2006-3542, Fluid Dynamics Conf., San Francisco, CA, 2006.

[8]Adrian, R., Christiansen, K., and Liu, Z., "Analysis and Interpretation of Instantaneous Velocity Fields," *Exp. Fluids*, Vol. 41, 2000, pp. 319–326.

[9]Graftieaux, L., Michard, M., and Grosjean, N., "Combining PIV, POD and Vortex Identification Algorithms for the Study of Unsteady Turbulent Swirling Flows," *Meas. Sci. Tech.*, Vol. 12, 2001, pp. 1422–1429.

[10]Mahesh, K., Constantinescu, G., and Moin, P., "A New Time-Accurate Finite-Volume Fractional-Step Algorithm for Prediction of Turbulent Flows on Unstructured Hybrid Meshes," *J. Comp. Phy.*, Vol. 197, 2004, pp. 215–240.

[11]Mahesh, K., Constantinescu, G., Apte, S,V, Iaccarino, G., Ham, F., and Moin, P., "Large-Eddy Simulation of Reacting Turbulent Flows in Complex Geometries," *ASME J. App. Mech.*, Vol. 438, 2006, pp. 101–128.

[12]Moin, P., and Apte, S.V., "Large Eddy Simulation of Multiphase Reacting Flows in Complex Combustors," *AIAA J. (special issue on 'Combustion Modeling and LES: Development and Validation Needs for Gas Turbine Combustors)*, Vol. 44, 2006, pp. 698–710.

[13]Apte, S. V., Mahesh, K., Moin, P., & Oefelein, J.C., "Large-Eddy Simulation of Swirling Particle-Laden Flows in a Coaxial-Jet Combustor," *Int. J. Mult. Flow*, Vol. 29, 2003a, pp. 1311–1331.

[14]Chen, Guoning and Lin, Zhongzang and Morse, Daniel and Snider, Stephen and Apte, Sourabh and Liburdy, James and Zhang, Eugene, "Multiscale feature detection in unsteady separated flows," *Accepted for publication in Int. J. of Numerical Analysis and Modeling*, 2008.

[15]Snider, Stephen and Morse, Daniel and Chen, Guoning and Apte, Sourabh V. and Liburdy, James A. and Zhang, Eugene, "Detection and analysis of separated flow induced vortical structures," *Proceedings of the AIAA ASM 2008*, AIAA-2008-0361, 2008.

[16]Lyn, D.A. and Einav, S. and Rodi, W. and Park, J.-H., "A laser-Doppler velocimetry study of ensemble-averaged characteristics of the turbulent near wake of a square cylinder," *J. Fluid Mech.*, Vol 304, 1995, pp 285–319.

[17]Rodi, W. and Ferziger, J.H. and Breuer, M. and Pourquié, M., "Status of large eddy simulation: results of a workshop," *Transactions of the ASME*, Vol. 119, 1997, pp. 248–262.

[18]Durão, D.F.G. and Heitor, M.V. and Pereira, J.C.F., "Measurements of turbulent and periodic flows around a square cross-section cylinder," *Experiments in Fluids*, Vol. 6, 1988, pp. 298–304.